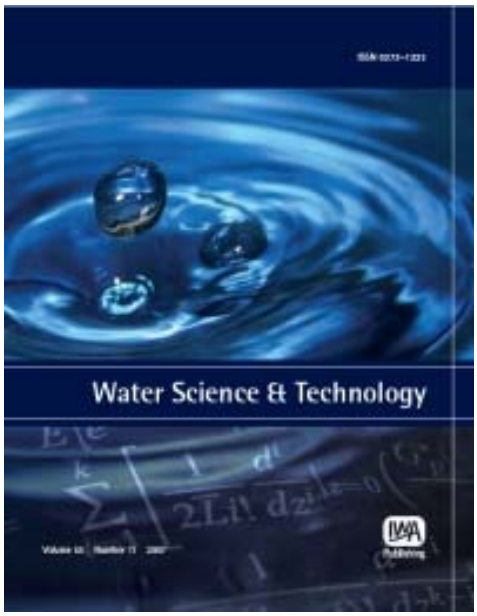

Quantum efficiencies of the photo-Fenton degradation of atrazine in water

T. B. Benzaquén, M. A. Isla and O. M. Alfano

ABSTRACT

An experimental work in a well-stirred batch recycling reactor for the photo-Fenton degradation of atrazine in water is presented. A study of the quantum efficiency is performed to assess the effectiveness of the photo-Fenton process on the atrazine degradation and total organic carbon (TOC) mineralization. Apparent and absolute quantum efficiencies of degradation and mineralization of an atrazine-based commercial herbicide are determined under different experimental conditions. Higher apparent efficiencies were found for both atrazine degradation and TOC mineralization when the ferric ion and hydrogen peroxide concentrations are increased. Because of the well known stability of the triazine ring, atrazine was not completely mineralized by the photo-Fenton process. However, a TOC reduction of 40% was achieved, being 62.5% of the maximum value that can be reached.

Key words | atrazine, photo-Fenton, quantum efficiencies

T. B. Benzaquén
M. A. Isla
O. M. Alfano (corresponding author)
INTEC (UNL- CONICET),
Ruta Nacional N° 168,
3000 Santa Fe,
Argentina
E-mail: *alfano@santafe-conicet.gov.ar*

M. A. Isla
O. M. Alfano
FICH, UNL,
3000 Santa Fe,
Argentina

INTRODUCTION

Atrazine, a member of the s-triazine group of herbicides, is one of the most commonly used herbicides in the world, mainly for pre- and post-emergence control of broadleaf and grassy weeds (EPA). Due to its relatively high aqueous solubility and bioresistance, atrazine enters easily and persists in soil and the aquatic environment (Krysova *et al.* 2003). Consequently, it is more frequently detected in water than any other herbicides in many countries.

Since 1980, atrazine was classified as a probable human carcinogen, and in recent times has been considered as an endocrine disruptor. The carcinogenic and toxic effects of s-triazines (Biradar & Rayburn 1995) of this herbicide have been extensively studied in drinking water (Cimino-Reale *et al.* 2008). Furthermore, it is known that it is a banned or regulated substance in several countries (Ackerman 2007).

In recent years, the use of advanced oxidation processes (AOPs) to treat contaminated wastewater has received considerable attention. The photo-Fenton process is one of the AOPs that has proven to be a promising method for the elimination of toxic and biologically nondegradable organic compounds (Pignatello *et al.* 2006). This process involves the use of hydrogen peroxide (oxidizing agent), iron salts (catalyst) and irradiation. The photo-Fenton process has several advantages compared with others AOPs; e.g. the reagents are readily available, simple to store, safe to handle, and non-aggressive to the environment. Furthermore, it is possible to employ solar radiation to activate the process, a fact that can significantly reduce the operational cost of the treatment.

The photodegradation of atrazine has been widely studied and it has proven to be effective to remove this pollutant from water (Chan & Chu 2006 and Chen *et al.* 2009). In this work, the photo-Fenton degradation and mineralization of the commercial herbicide atrazine was studied. For this purpose, a well-stirred batch reactor irradiated by UV-lamps was used. Furthermore, in order to assess the effectiveness of the herbicide degradation and compare the experimental results, quantum efficiencies were evaluated under different experimental conditions. For polychromatic radiation, both: (i) the apparent quantum efficiency, η_{app} (or the photonic efficiency); and (ii) the absolute quantum efficiency η_{abs} (or the quantum efficiency) have been evaluated.

QUANTUM EFFICIENCIES

The apparent quantum efficiency can be defined as the ratio of the number of reactant molecules degraded during a

doi: 10.2166/wst.2012.439

given time, to the total number of photons arriving at the reactor wall, during the same period of time. The apparent quantum efficiency (η_{app}) of atrazine degradation, can be expressed as (Salaices *et al.* 2002):

$$\eta_{ATZ,app} = \frac{\{reaction\ rate\ of\ atrazine\}}{\{rate\ of\ photon\ arriving\ at\ the\ reactor\ wall\}} \quad (1)$$

The absolute quantum efficiency can be defined as the ratio of the number of reactant molecules degraded during a given time to the total number of photons absorbed by the species to be activated, over the employed spectral range of wavelengths, during the same period of time (Cabrera *et al.* 1994 and Salaices *et al.* 2002). The absolute quantum efficiency (η_{abs}), can be defined as:

$$\eta_{ATZ,abs} = \frac{\{reaction\ rate\ of\ atrazine\}}{\{rate\ of\ photon\ absorbed\ by\ the\ species\ to\ be\ actived\}} \quad (2)$$

For this reacting system, Equations (1) and (2) can be expressed as:

$$\eta_{ATZ,\,app} = \frac{\left(C_{ATZ,t_0} - C_{ATZ,t_f}\right)V_T}{\langle q_W(x)\rangle_{A_W} A_W (t_f - t_0)} \quad (3)$$

and

$$\eta_{ATZ,\,abs} = \frac{\left(C_{ATZ,t_0} - C_{ATZ,t_f}\right)V_T}{\langle \sum_\lambda e^a_\lambda(x)\rangle_{V_R} V_R (t_f - t_0)} \quad (4)$$

where $(t_f - t_0)$ is the time length of the experimental run, V_R the reactor volume, V_T the total system volume, C_{ATZ} the molar concentration of atrazine, $\langle q_W(x)\rangle_{A_W}$ the incident radiation flux at the reactor window averaged over the window area (A_W), and $\langle \sum_\lambda e^a_\lambda(x)\rangle_{V_R}$ the local volumetric rate of photon absorption (LVRPA) averaged over the reactor volume (V_R). The expression $\left(C_{ATZ,t_0} - C_{ATZ,\,t_f}\right)/(t_f - t_0)$ in Equations (3) and (4) represents the atrazine oxidation rate.

With the purpose of considering the complete mineralization of the commercial herbicide, the conversion of the total organic carbon (TOC) should be evaluated. Thus, the mineralization quantum efficiencies, $\eta_{TOC,}$ can be expressed as (Satuf *et al.* 2007):

$$\eta_{TOC,\,app} = \frac{\{amount\ of\ TOC\ converted\}}{\{rate\ of\ photon\ arriving\ at\ the\ reactor\ wall\}} \quad (5)$$

and

$$\eta_{TOC,\,abs} = \frac{\{amount\ of\ TOC\ converted\}}{\{rate\ of\ photon\ absorbed\}} \quad (6)$$

In our reacting system, Equations (5) and (6) can be expressed as follows:

$$\eta_{TOC,\,app} = \frac{\left(TOC_{t_0} - TOC_{t_f}\right)V_T}{\langle q_W(x)\rangle_{A_W} A_W (t_f - t_0)} \quad (7)$$

and

$$\eta_{TOC,\,abs} = \frac{\left(TOC_{t_0} - TOC_{t_f}\right)V_T}{\langle \sum_\lambda e^a_\lambda(x)\rangle_{V_R} V_R (t_f - t_0)} \quad (8)$$

Here TOC represents the concentration of the total organic carbon as a function of time.

EXPERIMENTS

Chemicals

Atrazine ($C_8H_{14}ClN_5$, 90%, commercial formulation, SYNGENTA) was employed as the model pollutant. The experiments were performed employing iron sulfate (Carlo Erba, RPE), reagent-grade hydrogen peroxide (30% w/v, Ciccarelli p.a.) and concentrated sulfuric acid (95–98% Pro-analysis, Ciccarelli p.a.) for pH adjustment. The photo-treated solutions were neutralized by NaOH (reagent-grade, Mallinckrodt).

Set-up

The experimental device employed for the photo-Fenton degradation of atrazine was an isothermal, well-stirred batch recycling reactor. A scheme of the experimental device is presented in Figure 1. The flat-plate reactor made of borosilicate glass and circular cross section, was irradiated from both sides with two tubular lamps placed at the focal axis of two cylindrical reflectors of parabolic cross section. The radiant energy was supplied by two black light UV-lamps (TLK40W/09N, Philips). The lamps emit in the 315–400 nm range, with an emission peak at 365 nm.

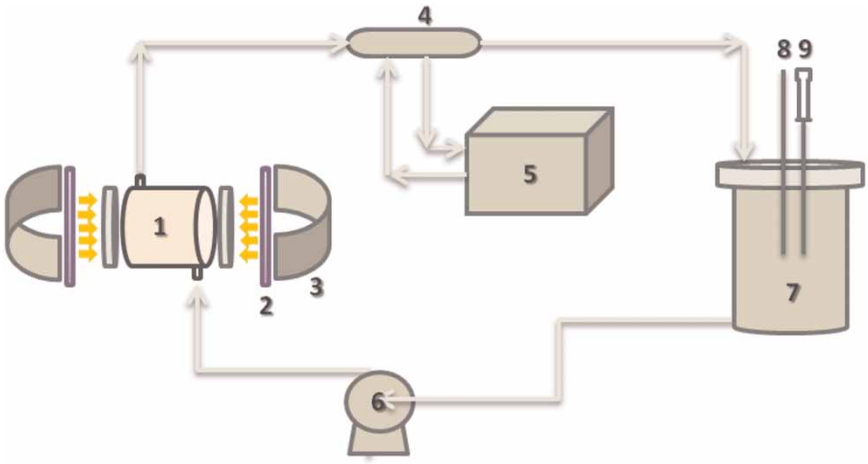

Figure 1 | Schematic representation of the experimental set up. Key: 1-photoreactor, 2-UV lamp, 3-parabolic reflector, 4-heat exchanger, 5-thermostatic bath, 6-pump, 7-storage tank, 8-thermometer, and 9-liquid sampling.

The system included a borosilicate glass storing tank, which was equipped with a liquid sampling valve, a thermometer and a pH control. Also, the experimental setup had an all-glass heat exchanger connected to a thermostatic bath, to keep the temperature constant during the reaction, and a centrifugal pump to achieve a high recirculating flow rate of the aqueous solution. The main characteristics and dimensions of the experimental set up are summarized in Table 1.

Procedure

Experimental runs began when the solutions of atrazine and iron sulfate were added to the storage tank with distilled water, and the pH was adjusted to 2.8–3.0 with concentrated sulfuric acid. Afterwards, the hydrogen peroxide solution was added and the reacting mixture was well homogenized by recirculation for 10 min at a flow rate of 83.3 $cm^3 s^{-1}$. The pump flow rate provided good mixing conditions. During this time interval, the UV-lamps were turned on with the aim of stabilizing the radiation emission. A shutter was located between each lamp and reactor window to avoid radiation entering at the reactor. Then the first sample was withdrawn and immediately the shutters were removed, defining the reaction time equal to zero. The temperature throughout the experiments was kept constant at 298 K and liquid samples were taken at equal time intervals (30 min).

Table 1 | Experimental set up

Reactor	Irradiated volume	69.94 cm^3
	Diameter	4.40 cm
	Length	4.60 cm
	Total liquid volume	3,000 cm^3
Lamps	Nominal power	40 W
	Output power: 315 nm $\leq \lambda \leq$ 400 nm	6.6 W
	Diameter	3.8 cm
	Nominal arc length	61 cm
Reflector	Parabola characteristic constant	2.75 cm
	Distance vertex of parabolic reflector to reactor plate	6.0 cm
	Length	50 cm
Pump	Flow rate	83.3 $cm^3 s^{-1}$
Thermostatic bath	Temperature	298 K

Analytical determinations

Atrazine concentration was measured using reverse phase liquid chromatography (flow rate 1 mL min^{-1}) with a UV detector (detection wavelength of 221 nm) in a HPLC-UV (Waters, Model Code 5CH) with C-18 column (X-Terra® RP) and employing acetonitrile/water (50/50) as the mobile phase. Hydrogen peroxide concentration was analyzed with a modified iodometric technique using a UV-VIS CARY 100 BIO, at 350 nm ($\varepsilon = 2.33 \times 10^4$ L mol^{-1} cm^{-1}) (Allen *et al.* 1952). Analysis of ferrous ions was performed with standard spectrophotometric techniques by means of absorbance measurements of the Fe(II)-phenantroline complex, $\varepsilon = 1.11 \times 10^4$ L mol^{-1} cm^{-1} at 510 nm (APHA 1995). The mineralization of the commercial herbicide was evaluated by means of TOC measurements with a Shimadzu TOC-5000A analyzer.

THE LOCAL VOLUMETRIC RATE OF PHOTON ABSORPTION

According to Equations (3) and (7), to determine the apparent quantum efficiencies is necessary to calculate the incident radiation flux at the reactor window. Similarly, to compute the absolute quantum efficiencies [Equations (4) and (8)] is necessary to know the LVRPA averaged over the reactor volume. To obtain e^a_λ, the radiation field inside the photoreactor must be assessed.

In a previous work, Alfano *et al.* (1985) proposed and experimentally validated a radiation field model for a similar emitting system. The authors have found that, for restricted optical and geometrical parameters, variations in the radial and angular coordinates did not yield significant changes in the LVPRA. Based on these results, a 1-D radiation field model has been used in this work to calculate the spectral LVRPA (Rossetti *et al.* 2002). Thus:

$$e^a_\lambda(x,t) = \kappa_\lambda(t)\, q_w\, f_\lambda \exp\left[-\kappa_{T,\lambda}(t)x\right] \tag{9}$$

Here x is the spatial coordinate, t the reaction time, q_w the net radiative flux at the reactor wall, f_λ the normalized spectral distribution of the lamp output power provided by the lamp manufacturer, κ_λ the reactant species absorption coefficient, and $\kappa_{T,\lambda}$ the total absorption coefficient. The spectral volumetric absorption coefficient of the reacting species is given by:

$$\kappa_\lambda(t) = \alpha_{Fe(OH)^{2+},\lambda} C_{Fe(OH)^{2+}}(t) \tag{10}$$

where $\alpha_{Fe(OH)^{2+},\lambda}$ is the molar absorptivity and $C_{Fe(OH)^{2+}}$ the molar concentration of the absorbing species [$Fe(OH)^{2+}$].

According to Faust & Hoigné (1990) the iron complex $Fe(OH)^{2+}$ is the dominant species at pH = 3. Besides, radiation absorption of ferrous ion (Fe^{2+}) and hydrogen peroxide (H_2O_2) is negligible for a wavelength $\lambda > 300$ nm. So:

$$\kappa_{T,\lambda} = \sum\nolimits_{\alpha i,\lambda} C_i(t) \cong \alpha_{Fe(OH)^{2+},\lambda} C_{Fe(OH)^{2+}}(t) \tag{11}$$

Note that, in the case of a flat-plate reactor of a circular cross section irradiated from both sides, similar expressions may be used for each emitting system. Then, when Equations (10) and (11) are substituted into Equation (9), the following expression may be written:

$$e^a_\lambda(x,t) = \alpha_{Fe(OH)^{2+},\lambda} C_{Fe(OH)^{2+}}(t)\, q_W\, f_\lambda \times \left\{\exp\left[-\alpha_{Fe(OH)^{2+},\lambda} C_{Fe(OH)^{2+}}(t)x\right] + \exp\left[-\alpha_{Fe(OH)^{2+},\lambda} C_{Fe(OH)^{2+}}(t)(L_R - x)\right]\right\} \tag{12}$$

Due to the fact that the incident UV-radiation is polychromatic and the optical properties of the radiation absorbing species are functions of wavelength, an integration over the wavelength range of interest must be performed. Thus:

$$\int_{\lambda_{min}}^{\lambda_{max}} e^a_\lambda(x,t)\,d\lambda \cong \sum_\lambda e^a_\lambda(x,t) \tag{13}$$

Finally, the LVRPA averaged over the reactor volume can be evaluated by:

$$\left\langle \sum_\lambda e^a_\lambda(x,t) \right\rangle = \sum_\lambda \frac{2\, q_W f_\lambda}{L}\left[1 - e^{\left(-\alpha_{Fe(OH)^{2+},\lambda} C_{Fe(OH)^{2+}}(t)\, L_R\right)}\right] \tag{14}$$

RESULTS

Degradation of atrazine by the photo-Fenton process under different operation conditions was investigated by keeping the initial atrazine concentration constant at 6.95×10^{-5} mol L^{-1} (equivalent to 15 ppm). The photooxidation reactions were planned according to a two-level factorial design. This set of experimental runs was performed using different values of the hydrogen peroxide to atrazine initial molar ratio (R) and ferric iron initial concentration (C^0_{Fe3+}). Table 2 presents a summary of the operating conditions for the experimental program.

The molar absorptivity of the $Fe(OH)^{2+}$(radiation absorbing species) as a function of the wavelength was taken from Faust & Hoigné (1990). The net radiative flux at the reactor walls (q_w) was measured using the potassium ferrioxalate actinometer (Murov *et al.* 1993). The same method was used to corroborate that the radiative flux at the radiation entrance takes on equal values from both sides. The net radiative flux at the reactor wall was determined to be 8.63×10^{-9} Einstein $cm^{-2}s^{-1}$.

It is well known that atrazine is not totally mineralized (Hincapié *et al.* 2006; Maldonado *et al.* 2007). These authors

Table 2 | Quantum efficiencies for the atrazine degradation and TOC mineralization

					Degradation quantum efficiency		Mineralization quantum efficiency	
R	$C^0_{Fe3+} \times 10^8$ (mol cm^{-3})	$\Delta C^a_{ATZ} \times 10^8$ (mol cm^{-3})	$\Delta TOC^b \times 10^9$ (mol cm^{-3})	$\langle e_a(x)\rangle_{V_R} \times 10^{10}$ (Einstein cm^{-3}s^{-1})	$\eta_{ATZ,app}$ (%)	$\eta_{ATZ,abs}$ (%)	$\eta^*_{TOC,app}$ (%)	$\eta^*_{TOC,abs}$ (%)
35	8.95	1.84	1.37	7.76	5.86	28.28	7.07	14.40
35	26.9	2.54	2.52	13.7	8.07	22.06	13.02	15.01
35	44.8	2.85	4.54	15.8	9.06	21.47	23.42	23.46
175	8.95	2.69	2.62	7.76	8.54	41.26	13.53	27.58
175	26.9	3.80	5.16	13.7	12.08	33.02	26.64	30.72
175	44.8	4.38	6.74	15.8	13.91	32.98	34.85	34.89
350	8.95	3.76	3.81	7.76	11.94	57.65	19.71	40.16
350	26.9	5.21	8.56	13.7	16.54	45.23	44.21	50.98
350	44.8	5.88	12.4	15.8	18.69	44.31	63.64	63.80

[a]$\Delta C_{ATZ} = C_{ATZ,t_0} - C_{ATZ,tf}$.
[b]$\Delta TOC = TOC_{t_0} - TOC_{tf}$.

refer to the final formation of very recalcitrant compounds, bearing 3/8 of the TOC of the original molecule of atrazine (Pelizzetti *et al*. 1990; Konstantinou & Albanis 2003). Thus, according to the expression: $(TOC_0 - TOC_f)/TOC_0 = (1 - 3/8) = 0.625$ the maximum value of mineralization that can be reached is 62.5%. Based on this fact Equations (7) and (8) should take into account the residual 3/8 of the initial organic carbon content. Consequently relative mineralization quantum efficiencies, η^*_{TOC} can be defined as:

$$\eta^*_{TOC,\,app} = \frac{\eta_{TOC,\,app}}{\eta_{TOC,\,app,\,3/8}} \times 100 \tag{15}$$

and

$$\eta^*_{TOC,\,abs} = \frac{\eta_{TOC,\,abs}}{\eta_{TOC,\,abs,\,3/8}} \times 100 \tag{16}$$

where $\eta_{TOC,\,app,3/8}$ and $\eta_{TOC,\,app,3/8}$ are determined to be 1.537×10^{-2} and 3.643×10^{-2} mol Einstein^{-1}, respectively.

In Table 2, values of $\eta_{ATZ,app}$ and $\eta_{ATZ,abs}$ calculated from Equations (3) and (4) respectively, are reported. The relative apparent and absolute quantum efficiencies of the mineralization process, calculated from Equations (15) and (16) respectively, are also shown.

One can observe that, for $R = 35$ (stoichiometric requirement) the atrazine degradation rates are low; however, a significant increase in atrazine conversion is reached when R is increased from 35 to 350. Under the experimental conditions employed in this work, we have not detected an optimal value for R. When the ferric iron concentration is increased from 8.95 to 44.8×10^{-5} mol L^{-1} (or 5 to 25 ppm), for a constant value of R, an increase of $\eta_{ATZ,app}$ and a decrease of $\eta_{ATZ,abs}$ is observed. It should be noted that for the latter efficiency, the increase of the LVRPA averaged over the reactor volume (denominator of Equation (4)) is higher than the slight increase of the atrazine degradation rate (numerator of Equation (4)). In other words, when iron concentration increases both the numerator and denominator of Equation (4) increase, although the denominator increases more rapidly. Furthermore, from the results summarized in Table 2, it can be observed that the absolute quantum efficiencies for atrazine degradation are in the 21–58% range. These values are about 3 to 5 larger than those obtained for the apparent quantum efficiencies.

The effects of R and C^0_{Fe3+} on the TOC overall degradation were also analyzed. Note that important changes of TOC degradation were observed when C^0_{Fe3+} was modified between 8.95 and 44.8×10^{-5} mol L^{-1} and R was changed from 35 to 350. In addition, one can observe that increasing the hydrogen peroxide to atrazine molar ratio, increases both $\eta^*_{TOC,\,app}$ and $\eta^*_{TOC,\,abs}$.

A 3D plot of degradation quantum efficiencies after a reaction time $t = 60$ min, and of the relative mineralization quantum efficiencies after a reaction time $t = 240$ min, as a function of R and C^0_{Fe3+}, are shown in Figures 2 and 3, respectively. Apparent quantum efficiencies and absolute quantum efficiencies results for atrazine degradation are depicted in Figures 2(a) and 2(b), respectively; the

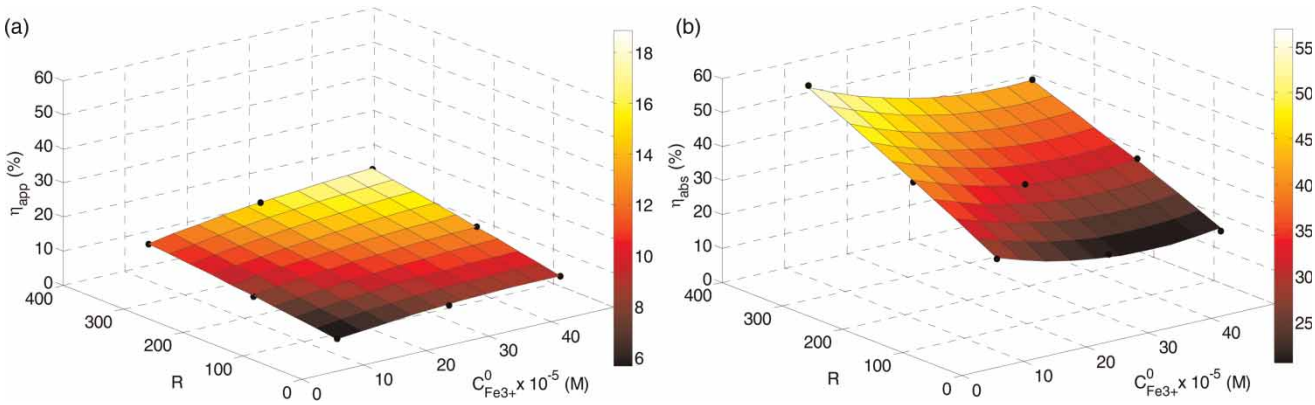

Figure 2 | Quantum efficiencies for the atrazine degradation. Key: (a) apparent efficiency and (b) absolute efficiency.

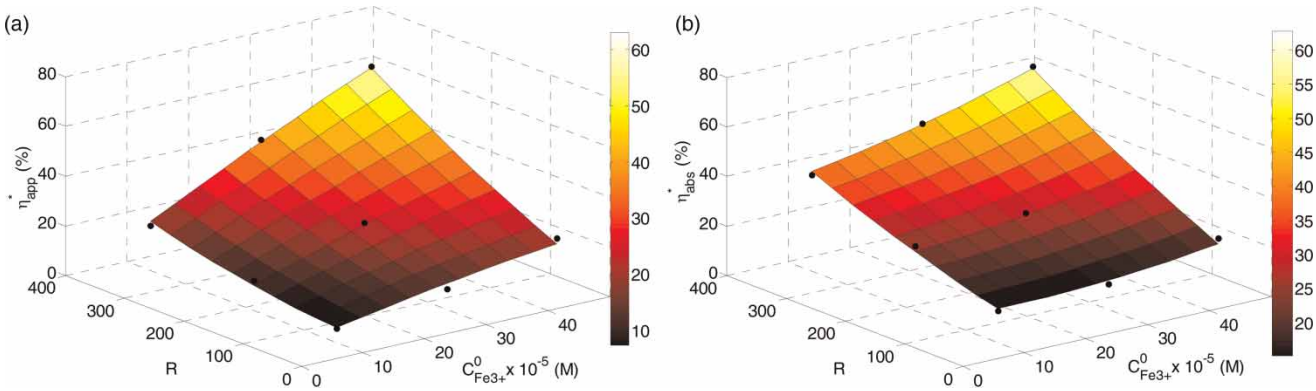

Figure 3 | Relative quantum efficiencies for the TOC mineralization. Key: (a) apparent efficiency and (b) absolute efficiency.

corresponding results of efficiencies for TOC mineralization are shown in Figures 3(a) and 3(b).

With reference to the TOC efficiencies, it is important to clarify that our photoreactor was able to reach a complete degradation of the atrazine in about 60 min (Figure 2), while a significant conversion of a TOC was only reached after 240 min (Figure 3). Hence, the mineralization quantum efficiencies show larger variations of the amount of TOC converted when compared with the changes of atrazine reaction rates. On the other hand, it should be noted that Figures 3(a) and 3(b) show 'relative' quantum efficiencies of mineralization, as was indicated in Equations (15) and (16). Taking into account that the maximum efficiency is only 62.5%, these figures present higher variations for apparent and absolute TOC efficiencies. These two facts can explain the higher sensitivity of the TOC efficiencies.

As mentioned above, atrazine is not completely mineralized by the photo-Fenton process due to the well known stability of the triazine ring (Hincapié *et al.* 2006 and Maldonado *et al.* 2007). In this work a TOC reduction of 40% was obtained through the photo-Fenton reaction. Cyanuric acid has been recognized as the final product of the atrazine degradation process (Pelizzetti *et al.* 1990). Furthermore, there is some evidence that cyanuric acid has low toxicity and is a biodegradable compound (Chan *et al.* 2004 and Lapertot *et al.* 2006). Consequently, these results suggest that the cyanuric acid could be subsequently eliminated in a biological treatment plant.

CONCLUSIONS

Quantum efficiencies of the photo-Fenton degradation of atrazine and TOC mineralization, in a well-stirred batch recycling reactor were evaluated. The influence of ferric iron initial concentration and hydrogen peroxide to atrazine initial concentration ratio on the degradation and mineralization processes has been determined. For each case, the

apparent and absolute quantum efficiencies were computed and compared.

We have found that when the ferric ion and hydrogen peroxide concentrations were increased, higher values of $\eta_{ATZ,app}$ were obtained. In contrast, the $\eta_{ATZ,abs}$ increased when the hydrogen peroxide to atrazine initial molar ratio was increased and the ferric iron concentration was decreased. This behavior is due to the absolute quantum efficiencies for the atrazine degradation depends strongly on the initial ferric ion concentration, unlike the apparent quantum efficiency, which does not change when the iron concentration is increased. It was found that the increase of the LVRPA averaged over the reactor volume ($\sum_\lambda e^a_\lambda(x)$), which is proportional to the increase of the iron concentration, was higher than the minor increase of the atrazine degradation rate. Consequently, the absolute quantum efficiency for atrazine was more sensitive to changes in the initial ferric iron concentration than the apparent quantum efficiency.

On the other hand, the apparent and absolute relative quantum efficiencies for TOC showed a higher sensitivity with respect to the apparent and absolute quantum efficiencies for atrazine degradation. Two factors can be used to explain this behavior: (i) the reaction times considered for the atrazine and TOC efficiencies are rather different; and (ii) the quantum efficiencies of mineralization were reported on a 'relative' basis, with a maximum TOC efficiency of 62.5%.

It is interesting to remark that atrazine is resistant to a complete mineralization by the photo-Fenton reaction, often observed for other substrates. Nevertheless, the TOC conversion was 40%, being 62.5% of the maximum value that can be achieved due to the stability of the triazine ring. The final product of the degradation, cyanuric acid, is biodegradable and with negligible toxicity; consequently, the cyanuric acid could be next eliminated in a biological treatment system.

ACKNOWLEDGEMENT

The authors are grateful to Universidad Nacional del Litoral (UNL), Consejo Nacional de Investigaciones Científicas y Técnicas (CONICET) and Agencia Nacional de Promoción Científica y Tecnológica (ANPCyT). They also thank Antonio C. Negro and Inés Curcio for their valuable help during the experimental work.

REFERENCES

Ackerman, F. 2007 The economics of atrazine. *International Journal of Occupational and Environmental Health* **13** (4), 437–445.

Alfano, O. M., Romero, R. L. & Cassano, A. E. 1985 A cylindrical photoreactor irradiated from the bottom – I. Radiation flux density generated by a tubular source and a parabolic reflector. *Chemical Engineering Science* **40** (11), 2119–2127.

Allen, A., Hochanadel, C., Ghormley, J. & Davis, J. 1952 Decomposition of water and aqueous solutions under mixed fast neutron and gamma radiation. *Journal of Physical Chemistry* **56**, 587–594.

APHA, AWWA, WEF 1995 *Standard Methods for the Examination of Water and Wastewater*, 19th edition. APHA, Washington, pp. 3–68.

Biradar, D. P. & Rayburn, A. L. 1995 Chromosomal damage induced by herbicide contamination at concentration observed in public water supplies. *Journal of Environmental Quality* **24** (6), 1232–1235.

Cimino-Reale, G., Ferrario, D., Casati, B., Brustio, R., Diodovich, C., Collotta, A., Vahter, M. & Gribaldo, L. 2008 Combined in-utero and juvenile exposure of mice to arsenate and atrazine in drinking water modulates gene expression and clonogenicity of myeloidprogenitors. *Toxicology Letters* **180** (1), 59–66.

Cabrera, M., Alfano, O. & Cassano, A. 1994 Novel reactor for photocatalytic kinetic studies. *Industrial and Engineering Chemistry Research* **33** (12), 3031–3042.

Chan, C. Y., Tao, S., Dawson, R. & Wong, P. K. 2004 Treatment of atrazine by integrating photocatalytic and biological processes. *Environmental Pollution* **131** (1), 45–54.

Chan, K. H. & Chu, W. 2006 Model applications and intermediates quantification of atrazine degradation by UV-enhanced Fenton process. *Journal of Agricultural and Food Chemistry* **54** (5), 1804–1813.

Chen, C., Yang, S., Guo, Y., Sun, C., Gu, C. & Xu, B. 2009 Photolytic destruction of endocrine disruptor atrazine in aqueous solution under UV irradiation: products and pathways. *Journal of Hazardous Materials* **172** (2–3), 675–684.

Faust, B. C. & Hoigne, J. 1990 Photolysis of Fe(III)-hydroxy complexes as sources of OH radicals in clouds, fog and rain. *Atmospheric Environment* **24A** (1), 79–89.

Hincapié, M., Peñuela, G., Maldonado, M., Malato, O., Fernández-Ibáñez, P., Oller, I., Gernjak, W. & Malato, S. 2006 Degradation of pesticides in water using solar advanced oxidation processes. *Applied Catalysis B: Environmental* **64** (3–4), 272–281.

Konstantinou, I. K. & Albanis, T. A. 2003 Photocatalytic transformation of pesticides in aqueous titanium dioxide suspensions using artificial and solar light: intermediates and degradation pathways. *Applied Catalysis B: Environmental* **42**, 319–335.

Krysova, H., Jirkovsky, J., Krysa, J., Mailhot, G. & Bolte, M. 2003 Comparative kinetic study of atrazine photodegradation in aqueous $Fe(ClO_4)_3$ solutions and TiO_2 suspensions. *Applied Catalysis B: Environmental* **40** (1), 1–12.

Lapertot, M., Pulgarin, C., Fernandez-Ibañez, M. I., Pérez-Estrada, L., Oller, I., Gernjak, W. & Malato, S. 2006 Enhancing biodegradability of priority substances (pesticides) by solar photo Fenton. *Water Research* **40** (5), 1086–1094.

Maldonado, M. I., Passarinho, P. C., Oller, I., Gernjak, W., Fernández, P., Blanco, J. & Malato, S. 2007 Photocatalytic degradation of EU priority substances: a comparison between TiO_2 and Fenton plus photo-Fenton in a solar pilot plant. *Journal of Photochemistry and Photobiology A: Chemistry* **185** (2–3), 354–363.

Murov, S. L., Carmichael, I. & Hug, G. L. 1993 *Handbook of Photochemistry*. 2nd edition, Marcel Dekker, New York.

Pignatello, J. J., Oliveros, E. & MacKay, A. 2006 Advanced oxidation processes for organic contaminant destruction based on the fenton reaction and related chemistry (Review). *Critical Reviews in Environmental Science and Technology* **36** (1), 1–84.

Pelizzetti, E., Maurino, V., Minero, C., Carlin, V., Pramauro, E., Zerbinati, O. & Tosato, M. L. 1990 Photocatalytic degradation of atrazine and other s-triazine herbicides. *Environmental Science and Technology* **24** (10), 1559–1565.

Rossetti, G. H., Albizzati, E. D. & Alfano, O. M. 2002 Decomposition of formic acid in a water solution employing the photo-fenton reaction. *Industrial and Engineering Chemistry Research* **41** (6), 1436–1444.

Salaices, M., Serrano, B. & de Lasa, H. I. 2002 Experimental evaluation of photon absorption in an aqueous TiO_2 slurry reactor. *Chemical Engineering Journal* **90** (3), 219.

Satuf, M. L., Brandi, R. J., Cassano, A. E. & Alfano, O. M. 2007 Quantum efficiencies of 4-chlorophenol photocatalytic degradation and mineralization in a well-mixed slurry reactor. *Industrial Engineering Chemical Research* **46** (1), 43–51.

First received 13 April 2012; accepted in revised form 15 June 2012